



1 An optimized tracer-based approach for estimating organic carbon emissions from
2 biomass burning in Ulaanbaatar, Mongolia

3

4 Jayant Nirmalkar¹, Tsatsral Batmunkh², Jinsang Jung^{1,*}

5 ¹Center for Gas Analysis, Korea Research Institute of Standards and Science
6 (KRISS), Daejeon 34113, Republic of Korea

7 ²Central Laboratory of Environment and Metrology, Ulaanbaatar, Mongolia

8

9 *Correspondence to: Jinsang Jung (jsjung@kriss.re.kr)*

10



11 **Abstract**

12 The impact of biomass burning (BB) on atmospheric particulate matter of $<2.5 \mu\text{m}$
13 diameter ($\text{PM}_{2.5}$) at Ulaanbaatar, Mongolia, was investigated using an optimized tracer-
14 based approach during winter and spring, 2017. Integrated 24 h $\text{PM}_{2.5}$ samples were
15 collected on quartz filters using a 30 L min^{-1} air sampler at an urban site in Ulaanbaatar.
16 The aerosol samples were analyzed for organic (OC) and elemental (EC) carbon,
17 anhydrosugars (levoglucosan, mannosan, and galactosan), and water-soluble ions. OC
18 was found to be the predominant species, contributing 64% and 56% to total aerosol
19 compositions in winter and spring, respectively. BB was identified as a major source of
20 $\text{PM}_{2.5}$, followed by dust and secondary aerosols. Levoglucosan/mannosan and
21 levoglucosan/ K^+ ratios indicate that softwood is the major fuel type in Ulaanbaatar.
22 Because of the large uncertainty associated with quantitative estimates of OC emitted
23 from BB (OC_{BB}), a novel approach was developed to optimize the OC/levoglucosan ratio
24 for estimating OC_{BB} . The optimum OC/levoglucosan ratio was obtained by regression
25 analysis between daily atmospheric concentrations of $\text{OC}_{\text{non-BB}}$ ($\text{OC}_{\text{total}} - \text{OC}_{\text{BB}}$) and
26 levoglucosan, with the softwood OC/levoglucosan ratio that gives the lowest correlation
27 coefficient (R^2) and slope in the regression analysis being treated as the optimum ratio.
28 The optimum OC/levoglucosan ratio was found to be 27.6 and 18.0 for winter and spring,
29 respectively, and these values were applied in quantifying OC_{BB} . It was found that 68%
30 and 63% of OC originated from BB during winter and spring, respectively. In addition to
31 OC_{BB} , sources of $\text{OC}_{\text{non-BB}}$ were investigated through multivariate correlation analysis,
32 and indicate that $\text{OC}_{\text{non-BB}}$ originated mainly from coal burning, vehicles, and vegetative
33 emissions.



34

35 **Keywords:** Source identification, Biomass burning, Optimized organic-
36 carbon/levoglucosan ratio

37

38



39 **1. Introduction**

40 Organic aerosol (OA; the organic fraction of particles) contributes a significant
41 fraction (10%–90%) of atmospheric particulate matter (PM), which can affect human
42 health and air quality (Jimenez et al., 2009; Maenhaut et al., 2011; Fu et al., 2012; Reche
43 et al., 2012; Chen et al., 2018). An understanding of the sources of PM is highly relevant
44 for air-quality remediation. Biomass burning (BB) is a major source of organic carbon
45 (OC) in PM_{2.5} (PM with aerodynamic diameter ≤ 2.5 μm) and it may become more
46 significant in future as air-quality regulations restrict other anthropogenic emissions
47 (Sullivan et al., 2019). Coal combustion, thermal power-plant, and traffic emissions also
48 make significant contributions to the OC content of PM (Watson et al., 2001a, b),
49 modifying PM characteristics such as hygroscopicity, light-attenuating properties, and
50 health impacts (Jung et al., 2009; Sullivan et al., 2019). Previous studies have observed
51 that the toxicity of PM_{2.5} increases with the oxidation potential of BB species because of
52 the water-soluble fraction of OC (Verma et al., 2014).

53 Previous studies have identified and quantified OC emitted from BB (OC_{BB}) using
54 the BB tracers (levoglucosan, mannosan, galactosan, and K⁺). Levoglucosan is produced
55 by the pyrolysis of cellulose at temperatures $>300^\circ\text{C}$ (Simoneit et al., 1999; Claeys et al.,
56 2010; Maenhaut et al., 2011; Nirmalkar et al., 2015; Achad et al., 2018); and two isomers
57 of levoglucosan, mannosan and galactosan, are produced by the burning of hemicellulose
58 (Reche et al., 2012). The atmospheric concentration of levoglucosan is higher than those
59 of the two isomers because of the lower content of hemicellulose (20%–30%, dry weight)
60 than cellulose (40%–50%) in softwood and hardwood (Reche et al., 2012; Sharma et al.,
61 2015). Water-soluble K⁺ can also be used as a BB tracer (Cheng et al., 2013; Nirmalkar
62 et al., 2015; Chen et al., 2018; Chantara et al., 2019). The proportion of these BB tracers



63 in PM depends on various factors such as the type of biomass (softwood, hardwood, crop,
64 grass, etc.), where it is burnt (traditional stoves, fireplaces, field burning, burning in
65 closed chambers, etc.), the type of burning (smoldering, flaming, etc.), and the burning
66 season (Fu et al., 2012; Cheng et al., 2013; Jung et al., 2014). Levoglucosan/mannosan,
67 levoglucosan/ K^+ , and OC/levoglucosan ratios were used to identify major biomass types
68 and quantify OC_{BB} in previous studies (Reche et al., 2012; Cheng et al., 2013; Jung et al.,
69 2014; Chen et al., 2018). However, OC/levoglucosan ratios are quite variable even with
70 the same type of BB because of variations in burning type, place, and season (Cheng et
71 al., 2013; Thepnuan et al., 2019 and references therein). It is therefore essential to
72 optimize the OC/levoglucosan ratio to better estimate OC_{BB} .

73 Ulaanbaatar, with a population of about 1 million, is an atmospheric pollution
74 ‘hotspot’ because of its topography, being situated in the Tuul river valley and surrounded
75 by the Khentei mountains, with a high elevation (1300 m–1949 m above sea level) and
76 large variations in temperature (-28°C to $+16^{\circ}\text{C}$) and relative humidity (17.7%–72.7%;
77 Table 1; Batmunkh et al., 2013; Jung et al., 2014). As the world’s coldest capital city
78 during winter, it requires additional fuel for space heating. The topography and low-
79 temperature conditions cause an increase in PM concentrations, which are exacerbated by
80 low wind speeds and atmospheric temperature inversions (Jung et al., 2010). Coal
81 consumption (~ 5 million tons per year) by 3 large power plants and 250 heat-only boilers
82 accounts for much of the anthropogenic OC emissions (Jung et al., 2010; Batmunkh et
83 al., 2013). Furthermore, about half of the population of Ulaanbaatar lives in traditional
84 Mongolian dwellings (Gers), with wood and coal being used for cooking and heating with
85 no pollution control devices (Jung et al., 2010; Batmunkh et al., 2013). About 93,000
86 motor vehicles are registered in Ulaanbaatar, with most being second-hand and with $\sim 80\%$



87 not satisfying current emission standards due to their age (54% are older than 11 years;
88 Jung et al., 2010; Batmunkh et al., 2013).

89 Few studies have investigated the chemical characteristics of organic aerosol in
90 Ulaanbaatar (Jung et al., 2010; Batmunkh et al., 2013), with none examining the
91 contribution of OC_{BB}. In this study, we quantified the BB tracers levoglucosan, mannosan,
92 galactosan, K⁺, and other chemical species. Potential sources of PM_{2.5} were identified by
93 principal component analysis (PCA), with levoglucosan/K⁺ and levoglucosan/mannosan
94 ratios being used to identify major biomass types.

95 OC_{BB} can be quantified from OC/levoglucosan ratios and levoglucosan
96 concentrations in PM. However, OC_{BB} uncertainties are large because OC/levoglucosan
97 ratios vary with fuel type, burning conditions, place, and type. Therefore, it is difficult to
98 determine the most suitable OC/levoglucosan ratio of BB emissions (Duan et al., 2004;
99 Cheng et al., 2013; Jung et al., 2014). Here, for perhaps the first time, optimized
100 OC/levoglucosan ratios were investigated for estimating concentrations of OC_{BB} during
101 winter and spring. OC_{non-BB} sources were also investigated using multivariate correlation
102 analysis with ions and elemental carbon (EC).

103

104 **2. Methods**

105 2.1 Sampling site and aerosol sampling

106 Aerosol sampling was carried out in Ulaanbaatar during the winter (17 January to 03
107 February) and spring (17 April to 4 May) of 2017, with 24 h periods commencing daily
108 at 11:00 local time. An aerosol sampler was installed on the rooftop of the National
109 Agency for Meteorology and Environmental Monitoring station in Ulaanbaatar (47°92'
110 N, 106°90' E), 10 m above ground level. The sampling site was located between



111 crossroads 8 km–10 km from two large thermal power plants to the west. PM_{2.5} samples
112 were collected on 47 mm diameter quartz filters (Pall-Life Sciences, USA) using an
113 aerosol sampler (Murata Keisokuki Service, Japan) at a flow rate of 30 L min⁻¹. Filters
114 were wrapped in aluminum foil and heated at 550°C for 12 h to remove adsorbed
115 impurities before use and stored at -20°C before and after sampling.

116

117 2.2 Filter analysis

118 A one-fourth part of quartz filter sample was extracted in 10 mL ultrapure water
119 (resistivity 18.2 MΩ, total OC content < 1 ppb,) under ultrasonication for 30 min. The
120 liquid was then filtered using a syringe filter (Millipore, Millex-GV, 0.45μm) and the
121 extract stored at 4°C pending analysis. Water-soluble cations (K⁺, Na⁺, Ca²⁺, Mg²⁺, and
122 NH₄⁺) were quantified by an ion chromatograph (Dionex ICS 5000, Thermo Fisher
123 Scientific, USA). Water-soluble cations were separated using an IonPac CS-12A column
124 (Thermo Fisher Scientific, USA) with 20 mM methanesulfonic acid as eluent at a flow
125 rate of 1.0 mL min⁻¹. Water-soluble anions (Cl⁻, NO₃⁻, and SO₄²⁻) were separated using
126 an IonPac AS-15 column (Thermo Fisher Scientific, USA) with 40 mM KOH as eluent
127 at a flow rate of 1.2 mL min⁻¹. The detection limits for major inorganic ions (based on 3σ
128 of blanks) were 0.01 μg m⁻³, 0.01 μg m⁻³, and 0.03 μg m⁻³ for NO₃⁻, SO₄²⁻, and NH₄⁺,
129 respectively.

130 Levoglucosan, mannosan, and galactosan were analyzed by a high-performance
131 anion-exchange chromatograph (Dionex, ICS-5000, Thermo Fisher Scientific, USA)
132 with pulsed amperometric detection involving an electrochemical detector with a gold
133 working electrode. Details of the method are given elsewhere (Jung et al., 2014). In brief,
134 separation involved a CarboPak MA1 (4 × 250 mm, Thermo Fisher Scientific, USA)



135 analytical column and NaOH eluent (360 mM, 0.4 mL min⁻¹). Limits of detection were
136 3.0 ng m⁻³, 0.7 ng m⁻³, and 1.0 ng m⁻³ for levoglucosan, mannosan, and galactosan,
137 respectively.

138 Aerosol samples were analyzed for OC and EC using a thermal optical OC/EC
139 analyzer (Sunset Laboratory Inc. Forest Grove, OR, USA) with laser transmittance-based
140 correction of pyrolysis. Details of the analyzer and quality-control parameters are
141 reported elsewhere (Jung et al., 2014). In brief, 1.5 cm² punch-core samples of quartz
142 filter were placed in a quartz dish inside the thermal desorption oven of the analyzer. OC
143 and EC were quantified using a temperature program developed by the US National
144 Institute for Occupational Safety and Health (NIOSH) in an inert atmosphere (100% He)
145 and in an oxidizing atmosphere (98% He + 2% O₂), respectively. Detection limits of OC
146 and EC were 0.04 and 0.01 μg C m⁻³, and analytical errors were 1.3% and 3.7%,
147 respectively.

148

149 **3. Results and Discussion**

150 **3.1 Chemical characteristics of PM_{2.5} and source identification**

151 Mass concentrations of carbonaceous aerosol, BB tracers, and water-soluble ions in
152 PM_{2.5} samples collected at Ulaanbaatar during winter and spring of 2017 are summarized
153 in Table 1. OC contributed 65% and 57% of the total chemical species quantified in winter
154 and spring, respectively (Table 1). Semi-volatile organic compounds (SVOCs)
155 condensation is generally favored by low-temperature conditions during winter in urban
156 atmospheres in China (Wang et al., 2018). Average concentrations of OC during winter
157 were five times those obtained in spring (Fig. 2). This may be attributed to additional BB
158 emission for home heating, increased condensation of SVOCs due to low temperatures,



159 and temperature inversions with low wind speeds (average wind speed $1.43 \pm 0.73 \text{ m s}^{-1}$;
160 Table 1 and Fig. 3a). During spring, OC concentrations increased with temperature ($R^2 =$
161 0.36 ; slope = 1.04) as shown in Fig. 3b, possibly due to volatilization of SVOCs during
162 periods of elevated temperature. A similar correlation between OC and temperature was
163 observed in the USA during the high-temperature months of 1998–2008 (Tai et al., 2010).
164 OC concentrations decreased with increasing wind speed during winter (Fig. 3a) and
165 spring (Fig. 3b), over all air temperature ranges. The inverse relationship between OC and
166 wind speed during winter (Fig. 3a) and spring (Fig. 3b) suggests a predominance of local
167 sources, with higher wind speeds flushing air pollutants out of the area whereas low wind
168 speeds allow them to accumulate (Khan et al., 2010).

169 Average concentration of EC during winter ($1.71 \pm 0.58 \mu\text{g m}^{-3}$) was higher than that
170 in spring ($1.11 \pm 0.42 \mu\text{g m}^{-3}$) (Table 1), consistent with general urban observations in
171 cities of China (Ji et al., 2016) and India (Panda et al., 2016). In winter and spring, EC
172 concentrations at the study site were lower than those observed in a suburban site ($2.3 \pm$
173 $1.0 \mu\text{g m}^{-3}$ and $3.1 \pm 1.5 \mu\text{g m}^{-3}$, respectively) and an urban site ($2.3 \pm 1.0 \mu\text{g m}^{-3}$ and 3.3
174 $\pm 1.2 \mu\text{g m}^{-3}$, respectively) in Shanghai, China (Feng et al., 2009). EC is emitted mainly
175 as primary particles during combustion and exists in an inert state in the atmosphere
176 (Zhang et al., 2015). Winter increases in EC concentration are therefore due mainly to
177 emissions from increased combustion of coal and biomass for space heating rather than
178 to effects of temperature and relative humidity. In spring, however, a strong correlation
179 was found between EC and temperature (Fig. 4; $R^2 = 0.81$), possibly due to increasing
180 temperature causing an increase in resuspension of EC with soil particles. This is
181 consistent with our observation of a strong correlation of Ca^{2+} concentration with
182 temperature ($R^2 = 0.83$; Fig. 4) and EC ($r = 0.90$; Table 4) during spring.



183 Daily concentrations of levoglucosan, mannosan and galactosan have similar trends
184 during winter and spring (Fig. 2), possibly because of combustion of similar biomass fuels
185 in both seasons. Changes in concentrations of these BB tracers might be attributed to
186 changes in relative proportions of cellulose and hemicellulose in different biomass fuels
187 (Zhu et al., 2015; Nirmalkar et al., 2015). Concentrations of anhydrosugars were four
188 times higher in winter than in spring (Table 1) due to increased heating requirements in
189 winter. The higher relative humidity (58.5%–72.7%) and lower temperature (−10.5°C to
190 −27.8°C; Table 1) in winter can also contribute to longer atmospheric residence times due
191 to increased levoglucosan stability (Lai et al., 2014). Higher concentrations of BB tracers
192 in winter than spring have previously been observed in Beijing, China, (Liang et al., 2016)
193 and were attributed to meteorological conditions similar to those of Ulaanbaatar.

194 Among water-soluble ions, SO_4^{2-} ($9.7 \pm 3.4 \mu\text{g m}^{-3}$) was the most dominant $\text{PM}_{2.5}$
195 species during winter, followed by NH_4^+ ($6.2 \pm 2.4 \mu\text{g m}^{-3}$) and NO_3^- ($4.2 \pm 1.7 \mu\text{g m}^{-3}$),
196 whereas SO_4^{2-} ($1.9 \pm 0.5 \mu\text{g m}^{-3}$) was the dominant species during spring, followed by
197 Ca^{2+} ($0.9 \pm 0.4 \mu\text{g m}^{-3}$) and NH_4^+ ($0.7 \pm 0.3 \mu\text{g m}^{-3}$). The total $\text{SO}_4^{2-} + \text{NH}_4^+ + \text{NO}_3^-$
198 content accounted for 27% and 23% of the total measured chemical species during winter
199 and spring, respectively (Fig. 2 and Table 1). SO_4^{2-} is the most prevalent water-soluble
200 ion in $\text{PM}_{2.5}$ in Wuhan, Guangzhou, and Tianjin (China) due to industrial emissions and
201 coal burning (Gu et al., 2011; Tao et al., 2014; Huang et al., 2016). This suggests that the
202 higher SO_4^{2-} concentration in Ulaanbaatar may be attributable to emissions from the three
203 major coal-fired thermal power plants near the study site.

204 The atmospheric concentrations of OC (11–17 $\mu\text{g m}^{-3}$) and levoglucosan (0.46–0.73
205 $\mu\text{g m}^{-3}$) were higher for samples collected during 27–30 April 2017 than on almost all
206 remaining days in spring (Fig. 2b). Backward atmospheric trajectories based on the



207 Hybrid Single-Particle Lagrangian Integrated Trajectory (HYSPLIT) model provided by
208 the US National Oceanic and Atmospheric Administration (NOAA) Air Resources
209 Laboratory (ARL) indicate that during those days air masses originated from a region
210 where a significant number of fires were detected [US Fire Information for Resource
211 Management System (FIRMS); National Aeronautics and Space Administration (NASA);
212 Fig. 5a, b)]. The elevated OC and levoglucosan concentrations during 27–30 April may
213 thus have been influenced by long-range transport from BB north of Mongolia.

214 Principal component analysis (PCA) is a useful tool for reducing the dimensionality
215 of large aerosol datasets to principal components using varimax rotation for source
216 identification (Cao et al., 2005; Lin et al., 2018; Nirmalkar et al., 2019). Four principal
217 components (PCs) in winter and three in spring were identified with eigenvalues >1
218 explaining 96% and 92%, respectively, of the total variance (Tables 2 and 3). The PCs
219 were categorized on the basis of loadings of chemical components as follows. In winter,
220 PC1 includes BB characterized by high loadings of levoglucosan, mannosan, and
221 galactosan; PC2 includes dust characterized by Ca^{2+} and Mg^{2+} content; PC3 includes
222 secondary formation characterized by SO_4^{2-} , NO_3^- , and NH_4^+ content; and PC4 includes
223 vehicular sources characterized by EC. In spring, PC1 includes BB (levoglucosan,
224 mannosan, and galactosan); PC2 includes dust (Ca^{2+} and Mg^{2+}) and vehicular emissions
225 (EC); and PC3 includes secondary formation (SO_4^{2-} , NO_3^- , and NH_4^+). In both in winter
226 and spring, BB was a major source of OC as indicated by high loadings of levoglucosan,
227 mannosan, and galactosan in PC1 (explaining 35% of the total variance). PCA results thus
228 indicate that BB is the major source of OC in Ulaanbaatar, with high positive loadings of
229 PC1 during both winter (0.82; Table 2) and spring (0.77; Table 3). Interestingly, the source
230 of K^+ changes with season, being associated with BB in winter (PC1 loading 0.70) and



231 dust re-suspension in spring (PC2 loading 0.65).

232

233 3.2 Relationship between BB tracers

234 The correlations among the three BB tracers levoglucosan, mannosan, and galactosan
235 are shown in Fig. 6a (winter) and 6b (spring). The correlations between levoglucosan and
236 mannosan and between levoglucosan and galactosan are strong during winter ($R^2 = 0.99$
237 for both pairs) and spring ($R^2 = 0.95$ and 0.83 , respectively; Fig. 6a, b). Concentrations of
238 levoglucosan and OC are strongly correlated in both winter ($R^2 = 0.78$) and spring ($R^2 =$
239 0.86 ; Fig. 7a), suggesting a major fraction of OC originates from BB in Ulaanbaatar. The
240 similar strong correlation and steep slope observed in OC–levoglucosan plots for PM
241 collected in Chiang Mai Province (Thailand) and Daejeon (Korea) were attributed mainly
242 to BB (Jung et al., 2014; Thepnuan et al., 2019). The substantial intercept values during
243 winter ($6.5 \mu\text{g C m}^{-3}$) and spring ($2.9 \mu\text{g C m}^{-3}$; Fig. 7a) can be explained by the emission
244 of OC from fossil-fuel combustion and other primary organic aerosol sources, and
245 secondary organic aerosol formation via gas–particle conversion in the atmosphere, with
246 the contribution of non-BB sources thus also being substantial.

247 The strong correlation between levoglucosan and K^+ concentrations ($R^2 = 0.68$) in
248 winter indicates they are produced from similar sources (Fig. 7b), with BB contributing
249 most of the K^+ . The higher concentration of K^+ in winter than spring in Hong Kong is
250 attributed to nearby residential and agricultural BB activities (Louie et al., 2005). At
251 Ulaanbaatar, the correlation between levoglucosan and K^+ is weaker in spring ($R^2 = 0.49$;
252 Fig. 7b), suggesting emission of K^+ from other sources together with BB. In spring, K^+
253 may be also derived from soil dust re-suspension due to
254 high wind speeds (up to 2.6 m s^{-1}) and dry atmospheric conditions ($\text{RH} = 35\%$) in



255 Ulaanbaatar (Table 1).

256 OC and K^+ concentrations are strongly correlated during winter ($R^2 = 0.79$; Fig. 8a)
257 and spring ($R^2 = 0.73$; Fig. 8b). As most of the aerosol particles emitted from BB occur
258 in $PM_{2.5}$, the correlation between OC and K^+ suggests that BB is one of the major sources
259 of ambient aerosol in Ulaanbaatar. The negative offset ($-6.88 \mu\text{g m}^{-3}$; Fig. 8a) during the
260 winter was due to an excess of K^+ . In winter, additional coal and wood are used for heating
261 and cooking in most traditional Ulaanbaatar houses (Batmunkh et al., 2013). Soil particles
262 present on the surface of coal and wood are unavoidably burned with the biomass.
263 Furthermore, the lignite coal commonly used for domestic purposes has a high ash content
264 (Batmunkh et al., 2013). Biomass and coal are burned in traditional stoves with no
265 pollution control devices (Batmunkh et al., 2013), so soil and ash particles are entrained
266 in convective processes and suspended in the atmosphere together with smoke particles
267 (Nirmalkar et al., 2019). The excess K^+ during winter may thus be due to the mixing of
268 BB and coal-burning particles with soil and ash particles.

269

270 3.3 Tracing the source of BB aerosol

271 OC is a major contributor to $PM_{2.5}$ during spring and winter in Ulaanbaatar, with
272 PCA indicating that BB is the major source of OC in both seasons. To quantify the OC_{BB} ,
273 it is necessary to identify the BB fuel type. Several investigators used
274 levoglucosan/mannosan and levoglucosan/ K^+ ratios to identify BB fuel types (Puxbaum
275 et al., 2007; Cheng et al., 2013; Jung et al., 2014; Chen et al., 2018; Thepnuan et al., 2019).

276 The levoglucosan/mannosan ratio is source-specific and may be used to identify BB
277 fuel types due to the unique cellulose and hemicellulose compositions of different
278 biomass fuels (Zhang et al., 2007; Cheng et al., 2013). A previous study suggested that



279 the levoglucosan/mannosan ratio is strongly dependent on wood type, rather than on the
280 site where the wood is grown (Cheng et al., 2013). Therefore, the levoglucosan/mannosan
281 ratio was used to trace the type of wood burnt during winter and spring for indoor heating
282 and cooking purposes. Previous studies have used levoglucosan/mannosan ratios to
283 investigate the BB fuel types (Cheng et al., 2013; Jung et al., 2014). However, the
284 levoglucosan/mannosan ratio cannot distinguish between emissions from crop residuals
285 (rice straw, wheat straw, and corn straw) and hardwood due to the overlap of ratios
286 between these fuel types (Cheng et al., 2013). However, levoglucosan/K⁺ ratio can
287 distinguish between the two groups (Jung et al., 2014, Chen et al., 2018). Both
288 levoglucosan/mannosan and levoglucosan/K⁺ ratios are therefore useful in distinguishing
289 various types of fuel (Cheng et al., 2013; Puxbaum et al., 2007).

290 A levoglucosan/mannosan–levoglucosan/K⁺ scatter plot based on results of the
291 present and previous studies is shown in Fig. 9, using data from Schauer et al. (2001),
292 Fine et al. (2001, 2002, 2004a, b), and Engling et al. (2006) for hardwood grown in the
293 USA; Schauer et al. (2001), Hays et al. (2002), Fine et al. (2001, 2002, 2004a, b), and
294 Engling et al. (2006) for US softwood; Schmidl et al. (2008), Bari et al. (2009) and
295 Goncalves et al. (2010) for hardwood grown in Europe; Iinuma et al. (2007), Schmidl et
296 al. (2008), and Goncalves et al. (2010) for European softwood; Engling et al. (2006) and
297 Sullivan et al. (2008) for needles and duff found in the USA; Sullivan et al. (2008) for US
298 grass; and from Sheesley et al. (2003), Sullivan et al. (2008), Engling et al. (2009) and
299 Oanh et al. (2011) for Asian rice straw.

300 The average levoglucosan/mannosan ratio was 3.6 ± 0.2 (range: 3.4 – 4.1) in winter
301 and 4.1 ± 1.0 (2.12 – 7.05) in spring, whereas the levoglucosan/K⁺ ratio was 8.9 ± 1.8
302 ($5.5 - 12.4$) in winter and 4.2 ± 2.1 (0.58 – 7.49) in spring at the study site (Fig. 9), within



303 the ranges reported for softwood burning sources (2.5 – 6.7 and 4.6 – 261, respectively)
304 (Fine et al., 2001; Schauer et al., 2001; Fine et al., 2002, 2004a, b; Hays et al., 2002;
305 Engling et al., 2006; Iinuma et al., 2007; Schmidl et al., 2008; Goncalves et al., 2010;
306 Cheng et al., 2013). During winter and spring, the levoglucosan/ K^+ and
307 levoglucosan/mannosan ratios thus appear in the softwood region (Fig. 9) for most of the
308 Ulaanbaatar ambient $PM_{2.5}$ samples analyzed in this study. Interestingly,
309 levoglucosan/mannosan ratios were similar in winter and spring, whereas the
310 levoglucosan/ K^+ ratio was significantly lower in spring. The most likely cause of the
311 similarity in levoglucosan/mannosan ratios is the use of similar types of domestic biofuels
312 (i.e., softwood; Fine et al., 2001, 2002; Cheng et al., 2013) all year around in Ulaanbaatar
313 (Batmunkh et al., 2013). Low levoglucosan/ K^+ ratios have been reported in aerosols from
314 crop-residue burning in China (Cheng et al., 2013) and South Korea (Jung et al., 2014),
315 and are likely due to the application of potassium fertilizers causing elevated K^+ levels in
316 the residues (Thepnuan et al., 2019). However, in Ulaanbaatar the lower levoglucosan/ K^+
317 ratios are due mainly to higher concentrations of levoglucosan in winter than spring with
318 K^+ concentrations being similar in both seasons (Fig. 9). Therefore, softwood burning
319 seems to be the major source of BB aerosol in Ulaanbaatar during both winter and spring,
320 consistent with previously reported softwood-burning emissions from fireplaces of
321 northern and southern regions of the USA (Fine et al., 2001, 2002), from household
322 combustion in Zhengzhou, China (Chen et al., 2018), and from stove wood combustion
323 in the mid-European region (Austria; Schmidl et al., 2008).

324

325 3.4 Optimization of OC/levoglucosan ratio for estimating OC_{BB} emission

326 OC_{BB} was estimated by multiplying OC/levoglucosan ratio and levoglucosan



327 concentration. Previous studies have used the OC/levoglucosan ratio obtained from
328 sources of BB aerosol to estimate OC_{BB} . A ratio of 7.35 reported for burning of four types
329 of US hardwood (Fine et al., 2002) was used for estimating OC_{BB} at four background sites
330 in Europe (Puxbaum et al., 2007). Later, mean value of 11.2 of OC/levoglucosan ratio
331 derived from ratios ranged between 4.5 – 24.6 was used for estimating OC_{BB} in the UK
332 (Harrison et al., 2012). However, such estimates may not be accurate as the
333 OC/levoglucosan ratio is highly variable in BB emissions. For example, the average
334 OC/levoglucosan ratio from softwood burning (23.8) is much higher than that of
335 hardwood burning (7.35) (Fine et al., 2002; Schmidl et al., 2008), differences are more
336 than ten-fold among studies of softwood-burning OC/levoglucosan ratios (Fine et al.,
337 2002; Hays et al., 2002; Engling et al., 2006; Iinuma et al., 2007; Goncalves et al., 2010).

338 Combustion conditions may also significantly influence OC/levoglucosan ratios. For
339 example, the OC/levoglucosan ratio varied by a factor of about seven between burning
340 the same wood (Loblolly pine) in a fireplace (27.6; Fine et al., 2002) and in a stove (3.4;
341 Fine et al., 2004b). The OC/levoglucosan ratio is also quite variable with a mean of 10.1
342 ± 7.97 in published data for softwood burning (range 1.90–27.6; Fig. 10). It is therefore
343 necessary to optimize the OC/levoglucosan ratio for use in estimating OC_{BB} . The large
344 variations in OC/levoglucosan ratios among emissions from different fuel types present a
345 major challenge, with the effects of burning conditions making it difficult to obtain the
346 most appropriate ratio for BB emissions at a given site.

347 Therefore, for the first time, we have used an optimized OC/levoglucosan ratio to
348 estimate precise concentration of OC_{BB} for the Ulaanbaatar study site. First, candidate
349 OC_{BB} in this study was estimated from OC/levoglucosan ratios for softwood burning in
350 the previous chamber experiment (Cheng et al., 2013 and papers cite therein) and



351 levoglucosan concentration in this site. Second, $OC_{\text{non-BB}}$ concentration was calculated by
352 subtracting OC_{BB} from corresponding total OC. If calculated $OC_{\text{non-BB}}$ doesn't contain
353 OC emitted from biomass burning, both regression slope and R^2 between $OC_{\text{non-BB}}$ versus
354 levoglucosan will be closed to zero. As shown in Fig. 11a and 11b, the lowest R^2 and
355 regression slope were observed when OC/levoglucosan ratios of 27.6 and 18.0 in winter
356 and spring, respectively. Thus, the optimized OC/levoglucosan ratios for our site were
357 determined to 27.6 and 18.0 in winter and spring, respectively.

358 The OC_{BB} concentrations at the Ulaanbaatar study site were calculated from the
359 optimized OC/levoglucosan ratios and levoglucosan concentrations. The OC_{BB}
360 concentration was estimated to be $33.1 \pm 11.9 \mu\text{g C m}^{-3}$ (range 16.0–58.5 $\mu\text{g C m}^{-3}$) and
361 $5.64 \pm 3.29 \mu\text{g C m}^{-3}$ (range 0.57–13.1 $\mu\text{g C m}^{-3}$), accounting for 68% and 63% of the
362 total OC in winter and spring, respectively (Fig. 12). The average of previously published
363 OC/levoglucosan ratios, 10.1 ± 7.9 (range 1.90 – 27.6), gives an estimated OC_{BB}
364 concentration of $12.1 \pm 4.4 \mu\text{g C m}^{-3}$ (range 5.9–21.4 $\mu\text{g C m}^{-3}$) and $3.2 \pm 1.8 \mu\text{g C m}^{-3}$
365 ($0.32\text{--}7.34 \mu\text{g C m}^{-3}$) in winter and spring, respectively. There values are 2.7 (winter) and
366 1.8 (spring) times lower than values estimated using our optimized OC/levoglucosan ratio.
367 Our estimated contribution of OC_{BB} was higher than that in Daejeon, South Korea (24%–
368 68% of total OC, mean $45\% \pm 12\%$; Jung et al., 2014) and Beijing, China (50% of total
369 OC; Cheng et al., 2013), where aerosols are produced mainly by the burning of crop
370 residues. The contribution of OC_{BB} to total OC is 57% and 31% during heating (average
371 temperature 0.6°C) and non-heating (average temperature 14°C) seasons in Krynica Zdroj,
372 Poland, significantly lower than that of Ulaanbaatar during both winter (average
373 temperature -21°C) and spring (average temperature 6°C). Such high concentrations of
374 OC_{BB} in Ulaanbaatar and Krynica Zdroj are likely to be due to intense wood burning for



375 heating during winter.

376

377 3.5 Tracing sources of $OC_{\text{non-BB}}$

378 A substantial contribution of $OC_{\text{non-BB}}$ to total OC was found during winter ($31\% \pm$
379 13%) and spring ($37\% \pm 20\%$; Fig. 12), with the similarity between seasons indicating
380 that $OC_{\text{non-BB}}$ originated mainly from local background sources. There is strong
381 correlation between $OC_{\text{non-BB}}$ and SO_4^{2-} , NH_4^+ , and K^+ in winter and $OC_{\text{non-BB}}$ and NO_3^- ,
382 Na^+ , K^+ , Mg^{2+} , Ca^{2+} , and EC in spring (Table 4). Residential combustion of coal emits
383 significant amounts of OC, EC, and inorganic species (SO_4^{2-} and metals) due to
384 incomplete combustion and lack of pollution control devices (Garcia et al., 1992; Li et
385 al., 2016; Watson et al., 2001a, b). Garcia et al. (1992) studied emissions of volatile
386 organic compounds from coal burning and vehicle engines. In Ulaanbaatar, the use of
387 coal for cooking and heating, and emissions from old vehicles are reported as major
388 sources of OC (Batmunkh et al., 2013). The three thermal power plants in Ulaanbaatar
389 are point sources for emissions of carbonaceous aerosol (Batmunkh et al., 2013), burning
390 ~ 5 million tons of coal per year (Batmunkh et al., 2013). High concentrations of anions
391 (SO_4^{2-} and NO_3^-) and cations (NH_4^+ and Na^+) are reported in China (Zhou et al., 2003),
392 the USA (Caiazzo et al., 2013), Brazil (Flues et al., 2002), India (Guttikunda et al., 2014),
393 Korea (Park et al., 2015), and Spain (Alastuey et al., 1999) near coal-fired thermal power
394 plants. Emissions of volatile organic compounds from vegetation have also been observed
395 in previous studies (Fehsenfeld et al., 1992; Shao et al., 2001; Acton et al., 2016). The
396 correlations of $OC_{\text{non-BB}}$ with ions and EC are thus likely due to volatile organic
397 compounds emitted from coal-burning and vehicles, and vegetative emissions.

398



399 **4. Conclusion**

400 BB was identified as a major source of $PM_{2.5}$ in Ulaanbaatar, Mongolia, during the
401 winter and spring of 2017, based on PCA. OC was the major component of $PM_{2.5}$ during
402 the entire sampling period, winter and spring. For determination of OC_{BB} , the fuel type
403 must be identified and levoglucosan/mannosan and levoglucosan/ K^+ ratios obtained from
404 previous studies and our on-site measurements were used for this purpose.

405 Softwood burning was identified as a major source of OC_{BB} . However,
406 OC/levoglucosan ratios from softwood burning are highly variable, and an optimum ratio
407 was derived by regression analysis between daily concentrations of OC_{non-BB} and
408 levoglucosan, yielding values of 27.6 and 18.0 for winter and spring, respectively. The
409 application of these ratios indicates that 68% and 63% of OC originated from BB during
410 winter and spring, respectively, which is about double that estimated using average values
411 of previous studies. The atmospheric concentration of OC_{BB} was higher in winter than
412 spring due mainly to additional BB for heating and cooking. BB aerosols in Ulaanbaatar
413 originate mainly from local softwood burning. The approach developed here may be
414 applied elsewhere for screening region-specific OC/levoglucosan ratios for estimating
415 atmospheric appropriate concentrations of OC_{BB} , aiding the establishment of BB control
416 measures.

417

418 **Author contribution**

419 Jinsang Jung and Batmunkh Tsatsral designed the study and carried out the field work.
420 Jinsang Jung performed chemical analyses and quality-control measures. Jayant
421 Nirmalkar wrote the manuscript under the guidance of Jinsang Jung. All authors



422 commented on and discussed the manuscript.

423

424 **Competing interests**

425 The authors declare that they have no conflict of interests.

426

427 **Acknowledgments**

428 This work was funded by a grant (19011057) from the Korea Research Institute of
429 Standards and Science (KRISS) under the Basic R&D Project of Quantification of local
430 and long-range transported pollutants during a severe haze episode over the Korean
431 Peninsula. The authors gratefully acknowledge the NOAA Air Resources Laboratory for
432 the provision of the HYSPLIT transport and dispersion model and access to the READY
433 website (<http://www.arl.noaa.gov/ready.html>) and the Fire Information for Resource
434 Management System (FIRMS) of the National Aeronautics and Space Administration
435 (NASA), United States (<https://firms.modaps.eosdis.nasa.gov/alerts/>) used in this study.

436

437 **Data availability**

438 The data used in this study are available from the corresponding author upon request
439 (jsjung@kriss.re.kr).

440

441



442 **References**

- 443 Achad, M., Caumo, S., de Castro Vasconcellos, P., Bajano, H., Gómez, D., and
444 Smichowski, P.: Chemical markers of biomass burning: Determination of
445 levoglucosan, and potassium in size-classified atmospheric aerosols collected in
446 Buenos Aires, Argentina by different analytical techniques, *Microchemical J.*, 139,
447 181–187, <https://doi.org/10.1016/j.microc.2018.02.016>, 2018.
- 448 Acton, W. J. F., Schallhart, S., Langford, B., Valach, A., Rantala, P., Fares, S., and Carriero,
449 G.: Canopy-scale flux measurements and bottom-up emission estimates of volatile
450 organic compounds from a mixed oak and hornbeam forest in northern Italy, *Atmos.*
451 *Chem. Phys.*, 16, 7149–7170, <https://doi.org/10.5194/acp-16-7149-2016>, 2016.
- 452 Alastuey, A., Querol, X., Chaves, A., Ruiz, C. R., Carratala, A., and Lopez-Soler, A.:
453 Bulk deposition in a rural area located around a large coal-fired power station,
454 northeast Spain, *Environ. Pollut.*, 106(3), 359–367, [https://doi.org/10.1016/S0269-](https://doi.org/10.1016/S0269-7491(99)00103-7)
455 [7491\(99\)00103-7](https://doi.org/10.1016/S0269-7491(99)00103-7), 1999.
- 456 Bari, M. A., Baumbach, G., Kuch, B., and Scheffknecht, G.: Wood smoke as a source of
457 particle-phase organic compounds in residential areas, *Atmos. Environ.*, 43,
458 4722–4732, <https://doi.org/10.1016/j.atmosenv.2008.09.006>, 2009.
- 459 Batmunkh, T., Kim, Y. J., Jung, J. S., Park, K., and Tumendemberel, B.: Chemical
460 characteristics of fine particulate matters measured during severe winter haze
461 events in Ulaanbaatar, Mongolia, *J. Air & Waste Manag. Assoc.*, 63, 659–670,
462 <https://doi.org/10.1080/10962247.2013.776997>, 2013.
- 463 Caiazzo, F., Ashok, A., Waitz, I. A., Yim, S. H., and Barrett, S. R.: Air pollution and early
464 deaths in the United States. Part I: Quantifying the impact of major sectors in 2005,
465 *Atmos. Environ.*, 79, 198–208, <https://doi.org/10.1016/j.atmosenv.2013.05.081>,
466 2013.
- 467 Cao, J. J., Wu, F., Chow, J. C., Lee, S. C., Li, Y., Chen, S. W., An, Z. S., Fung, K. K.,
468 Watson, J. G., Zhu, C. S., and Liu, S. X.: Characterization and source apportionment
469 of atmospheric organic and elemental carbon during fall and winter of 2003 in Xi'an,
470 China, *Atmos. Chem. Phys.*, 5, 3127–3137, [https://doi.org/10.5194/acp-5-3127-](https://doi.org/10.5194/acp-5-3127-2005)
471 [2005](https://doi.org/10.5194/acp-5-3127-2005), 2005.
- 472 Chantara, S., Thepnuan, D., Wiriya, W., Prawan, S., and Tsai, Y. I.: Emissions of pollutant
473 gases, fine particulate matters and their significant tracers from biomass burning in



- 474 an open-system combustion chamber, *Chemosphere*, 224, 407–416, 2019.
- 475 Chen, H., Yin, S., Li, X., Wang, J., and Zhang, R.: Analyses of biomass burning
476 contribution to aerosol in Zhengzhou during wheat harvest season in 2015, *Atmos.*
477 *Res.*, 207, 62–73, <https://doi.org/10.1016/j.atmosres.2018.02.025>, 2018.
- 478 Cheng, Y., Engling, G., He, K.-B., Duan, F.-K., Ma, Y.-L., Du, Z.-Y., Liu, J.-M., Zheng,
479 M., and Weber, R. J.: Biomass burning contribution to Beijing aerosol, *Atmos.*
480 *Chem. Phys.*, 13, 7765–7781, <https://doi.org/10.5194/acp-13-7765-2013>, 2013.
- 481 Claeys, M., Kourtchev, I., Pashynska, V., Vas, G., Vermeylen, R., Wang, W., Cafmeyer,
482 J., Chi, X., Artaxo, P., Andreae, M. O., and Maenhaut, W.: Polar organic marker
483 compounds in atmospheric aerosols during the LBA-SMOCC 2002 biomass
484 burning experiment in Rondônia, Brazil: sources and source processes, time series,
485 diel variations and size distributions, *Atmos. Chem. Phys.*, 10, 9319–9331,
486 <https://doi.org/10.5194/acp-10-9319-2010>, 2010.
- 487 Duan, F., Liu, X., Yu, T., Cachier, H.: Identification and estimate of biomass burning
488 contribution to the urban aerosol organic carbon concentrations in Beijing, *Atmos.*
489 *Environ.* 38, 1275–1282, <https://doi.org/10.1016/j.atmosenv.2003.11.037>, 2004
- 490 Engling, G., Carrico, C. M., Kreidenweis, S. M., Collett Jr., J. L., Day, D. E., Malm, W.
491 C., Lincoln, L., Hao, W. M., Iinuma, Y., and Herrmann, H.: Determination of
492 levoglucosan in biomass combustion aerosol by high-performance anion-exchange
493 chromatography with pulsed amperometric detection, *Atmos. Environ.*, 40,
494 299–311, <https://doi.org/10.1016/j.atmosenv.2005.12.069>, 2006.
- 495 Engling, G., Lee, J. J., Tsai, Y. W., Lung, S. C. C., Chou, C. C. K., Chan, C. Y.: Size
496 resolved anhydrosugar composition in smoke aerosol from controlled field burning
497 of rice straw, *Aerosol Sci. Technol.*, 43, 662–672,
498 <https://doi.org/10.1080/0278682090282511>, 2009.
- 499 Fehsenfeld, F., Calvert, J., Fall, R., Goldan, P., Guenther, A. B., Hewitt, C. N., Lamb, B.,
500 Liu, S., Trainer, M., Westberg, H., and Zimmerman, P.: Emissions of volatile
501 organic compounds from vegetation and the implications for atmospheric chemistry,
502 *Global Biogeochem. Cy.*, 6, 389–430, <https://doi.org/10.1029/92GB02125>, 1992.
- 503 Feng, Y., Chen, Y., Guo, H., Zhi, G., Xiong, S., Li, J., Sheng, G., and Fu, J.: Characteristics
504 of organic and elemental carbon in PM_{2.5} samples in Shanghai, China. *Atmos. Res.*,
505 92, 434–442, <https://doi.org/10.1016/j.atmosres.2009.01.003>, 2009.



- 506 Fine, P. M., Cass, G. R., and Simoneit, B. R. T.: Chemical characterization of fine particle
507 emissions from fireplace combustion of woods grown in the northeastern United
508 States, *Environ. Sci. Technol.*, 35, 2665–2675, <https://doi.org/10.1021/es001466k>,
509 2001.
- 510 Fine, P. M., Cass, G. R., and Simoneit, B. R. T.: Chemical characterization of fine particle
511 emissions from the fireplace combustion of woods grown in the southern United
512 States, *Environ. Sci. Technol.*, 36, 1442–1451, <https://doi.org/10.1021/es0108988>,
513 2002.
- 514 Fine, P. M., Cass, G. R., and Simoneit, B. R. T.: Chemical characterization of fine particle
515 emissions from the fireplace combustion of wood types grown in the midwestern
516 and western United States, *Environ. Engin. Sci.*, 21, 387–409,
517 <https://doi.org/10.1089/109287504323067021>, 2004a.
- 518 Fine, P. M., Cass, G. R., and Simoneit, B. R. T.: Chemical characterization of fine particle
519 emissions from the wood stove combustion of prevalent United States tree species,
520 *Environ. Engin. Sci.*, 21, 705–721, <https://doi.org/10.1089/ees.2004.21.705>, 2004b.
- 521 Flues, M., Hama, P., Lemes, M. J. L., Dantas, E. S. K., and Fornaro, A.: Evaluation of the
522 rainwater acidity of a rural region due to a coal-fired power plant in Brazil, *Atmos.*
523 *Environ.*, 36, 2397–2404, [https://doi.org/10.1016/S1352-2310\(01\)00563-5](https://doi.org/10.1016/S1352-2310(01)00563-5), 2002.
- 524 Fu, P. Q., Kawamura, K., Chen, J., Li, J., Sun, Y. L., Liu, Y., Tachibana, E., Aggarwal, S.
525 G., Okuzawa, K., Tanimoto, H., and Kanaya, Y.: Diurnal variations of organic
526 molecular tracers and stable carbon isotopic composition in atmospheric aerosols
527 over Mt. Tai in the North China Plain: an influence of biomass burning, *Atmos.*
528 *Chem. Phys.*, 12, 8359–8375, doi:10.5194/acp-12-8359-2012, 2012.
- 529 Garcia, J., Beyne-Masclat, S., Mouvier, G., and Masclat, P.: Emissions of volatile organic
530 compounds by coal-fired power stations. *Atmos. Environ. Part A. General Topics*,
531 26, 1589–1597, [https://doi.org/10.1016/0960-1686\(92\)90059-T](https://doi.org/10.1016/0960-1686(92)90059-T), 1992.
- 532 Gonçalves, C., Alves, C., Evtyugina, M., Mirante, F., Pio, C., Caseiro, A., Schmidl, C.,
533 Bauer, H., and Carvalho, F.: Characterisation of PM₁₀ emissions from wood stove
534 combustion of common woods grown in Portugal, *Atmos. Environ.*, 44, 4474–4480,
535 <https://doi.org/10.1016/j.atmosenv.2010.07.026>, 2010.
- 536 Gu, J., Bai, Z., Li, W., Wu, L., Liu, A., Dong, H., and Xie, Y.: Chemical composition of
537 PM_{2.5} during winter in Tianjin, China, *Particuology*, 9, 215–221,



- 538 <https://doi.org/10.1016/j.partic.2011.03.001>, 2011.
- 539 Guttikunda, S. K., and Jawahar, P.: Atmospheric emissions and pollution from the
540 coal-fired thermal power plants in India. *Atmos. Environ.*, 92, 449–460,
541 <https://doi.org/10.1016/j.atmosenv.2014.04.057>, 2014.
- 542 Harrison, R. M., Beddows, D. C. S., Hu, L., and Yin, J.: Comparison of methods for
543 evaluation of wood smoke and estimation of UK ambient concentrations, *Atmos.*
544 *Chem. Phys.*, 12, 8271–8283, doi:10.5194/acp-12-8271-2012, 2012.
- 545 Hays, M. D., Geron, C. D., Linna, K. J., Smith, N. D., and Schauer, J. J.: Speciation of
546 gasphase and fine particle emissions from burning of foliar fuels, *Environ. Sci.*
547 *Technol.*, 36, 2281–2295, <https://doi.org/10.1021/es0111683>, 2002.
- 548 Huang, X., Liu, Z., Zhang, J., Wen, T., Ji, D., Wang, Y.: Seasonal variation and secondary
549 formation of size-segregated aerosol water-soluble inorganic ions during pollution
550 episodes in Beijing, *Atmos. Res.*, 168, 70–79,
551 <https://doi.org/10.1016/j.atmosres.2015.08.021>, 2016.
- 552 Inuma, Y., Brüggemann, E., Gnauk, T., Müller, K., Andreae, M. O., Helas, G., Parmar,
553 R., and Herrmann, H.: Source characterization of biomass burning particles: the
554 combustion of selected European conifers, African hardwood, savanna grass, and
555 German and Indonesian peat, *J Geophys. Res.*, 112, D08209.
556 <http://dx.doi.org/10.1029/2006JD007120>, 2007.
- 557 Ji, D., Zhang, J., He, J., Wang, X., Pang, B., Liu, Z., Wang, L., and Wang, Y.:
558 Characteristics of atmospheric organic and elemental carbon aerosols in urban
559 Beijing, China. *Atmos. Environ.*, 125, 293–306,
560 <https://doi.org/10.1016/j.atmosenv.2015.11.020>, 2016.
- 561 Jimenez, J. L., Canagaratna, M. R., Donahue, N. M., Prevot, A. S. H., Zhang, Q., Kroll,
562 J. H., DeCarlo, P. F., Allan, J. D., Coe, H., Ng, N. L., and Aiken, A. C.: Evolution
563 of organic aerosols in the atmosphere, *Science*, 326, 1525–1529,
564 doi:10.1126/science.1180353, 2009.
- 565 Jung, J., Lee, H., Kim, Y. J., Liu, X., Zhang, Y., Hu, M., and Sugimoto, N.: Optical
566 properties of atmospheric aerosols obtained by in situ and remote measurements
567 during 2006 Campaign of Air Quality Research in Beijing (CAREBeijing-2006). *J.*
568 *Geophys. Res.: Atmos.*, 114(D2), <https://doi.org/10.1029/2008JD010337>, 2009.
- 569 Jung, J., Lee, S., Kim, H., Kim, D., Lee, H., and Oh, S.: Quantitative determination of the



- 570 biomass-burning contribution to atmospheric carbonaceous aerosols in Daejeon,
571 Korea, during the rice-harvest period, *Atmos. Environ.*, 89, 642–650,
572 <https://doi.org/10.1016/j.atmosenv.2014.03.010>, 2014.
- 573 Jung, J., Tsatsral, B., Kim, Y. J., and Kawamura, K.: Organic and inorganic aerosol
574 compositions in Ulaanbaatar, Mongolia, during the cold winter of 2007 to 2008:
575 dicarboxylic acids, ketocarboxylic acids, and α -dicarbonyls, *J Geophys. Res.:*
576 *Atmos.*, 115(D22), <https://doi.org/10.1029/2010JD014339>, 2010.
- 577 Khan, M. F., Shirasuna, Y., Hirano, K., and Masunaga, S.: Characterization of PM_{2.5},
578 PM_{2.5-10} and PM_{>10} in ambient air, Yokohama, Japan, *Atmos. Res.*, 96, 159–172,
579 <https://doi.org/10.1016/j.atmosres.2009.12.009>, 2010.
- 580 Lai, C., Liu, Y., Ma, J., Ma, Q., and He, H.: Degradation kinetics of levoglucosan initiated
581 by hydroxyl radical under different environmental conditions, *Atmos. Environ.*, 91,
582 32–39, <https://doi.org/10.1016/j.atmosenv.2014.03.054>, 2014.
- 583 Li, Q., Jiang, J., Zhang, Q., Zhou, W., Cai, S., Duan, L., Ge, S., and Hao, J.: Influences of
584 coal size, volatile matter content, and additive on primary particulate matter
585 emissions from household stove combustion. *Fuel*, 182, 780–787,
586 <https://doi.org/10.1016/j.fuel.2016.06.059>, 2016.
- 587 Liang, L., Engling, G., Du, Z., Cheng, Y., Duan, F., Liu, X., and He, K.: Seasonal
588 variations and source estimation of saccharides in atmospheric particulate matter in
589 Beijing, China, *Chemosphere*, 150, 365–377,
590 <https://doi.org/10.1016/j.chemosphere.2016.02.002>, 2016.
- 591 Lin, Y.-C., Hsu, S.-C., Lin, C.-Y., Lin, S.-H., Huang, Y.-T., Chang, Y., and Zhang, Y.-L.:
592 Enhancements of airborne particulate arsenic over the subtropical free troposphere:
593 impact of southern Asian biomass burning, *Atmos. Chem. Phys.*, 18, 13865–13879,
594 <https://doi.org/10.5194/acp-18-13865-2018>, 2018.
- 595 Louie, P. K., Watson, J. G., Chow, J. C., Chen, A., Sin, D. W. and Lau, A. K.: Seasonal
596 characteristics and regional transport of PM_{2.5} in Hong Kong, *Atmos. Environ.*, 39,
597 1695–1710, <https://doi.org/10.1016/j.atmosenv.2004.11.017>, 2005.
- 598 Maenhaut, W., Nava, S., Lucarelli, F., Wang, W., Chi, X., and Kulmala, M.: Chemical
599 composition, impact from biomass burning, and mass closure for PM_{2.5} and PM₁₀
600 aerosols at Hyytiälä, Finland, in summer 2007, *X-Ray Spectrometry*, 40, 168–171,
601 <https://doi.org/10.1002/xrs.1302>, 2011.



- 602 Nirmalkar, J., Deshmukh, D. K., Deb, M. K., Tsai, Y. I., and Pervez, S.: Characteristics of
603 aerosol during major biomass burning events over eastern central India in winter:
604 A tracer-based approach, *Atmos. Pollut. Res.*, 10, 817–826,
605 <https://doi.org/10.1016/j.apr.2018.12.010>, 2019.
- 606 Nirmalkar, J., Deshmukh, D. K., Deb, M. K., Tsai, Y. I., and Sopajaree, K.: Mass loading
607 and episodic variation of molecular markers in PM_{2.5} aerosols over a rural area in
608 eastern central India, *Atmos. Environ.*, 117, 41–50,
609 <https://doi.org/10.1016/j.atmosenv.2015.07.003>, 2015.
- 610 Oanh, N. T. K., Ly, B. T., Tipayarom, D., Manandhar, B. R., Prapat, P., Simpson, C.D.,
611 and Liu, L.J.S.: Characterization of particulate matter emission from open burning
612 of rice straw, *Atmos. Environ.*, 45, 493–502,
613 <https://doi.org/10.1016/j.atmosenv.2010.09.023>, 2011.
- 614 Panda, S., Sharma, S. K., Mahapatra, P. S., Panda, U., Rath, S., Mahapatra, M., Mandal,
615 T. K., and Das, T.: Organic and elemental carbon variation in PM_{2.5} over megacity
616 Delhi and Bhubaneswar, a semi-urban coastal site in India, *Nat. Hazards*, 80,
617 1709–1728, <https://doi.org/10.1007/s11069-015-2049-3>, 2016.
- 618 Park, S. M., Seo, B. K., Lee, G., Kahng, S. H., and Jang, Y.: Chemical composition of
619 water-soluble inorganic species in precipitation at Shihwa Basin, Korea,
620 *Atmosphere*, 6, 732–750, <https://doi.org/10.3390/atmos6060732>, 2015.
- 621 Pio, C. A., Legrand, M., Alves, C. A., Oliveira, T., Afonso, J., Caseiro, A., Puxbaum, H.,
622 Sanchez-Ochoa, A. and Gelencser, A.: Chemical composition of atmospheric
623 aerosols during the 2003 summer intense forest fire period, *Atmos. Environ.*, 42,
624 7530–7543, <https://doi.org/10.1016/j.atmosenv.2008.05.032>, 2008.
- 625 Puxbaum, H., Caseiro, A., Sánchez-Ochoa, A., Kasper-Giebl, A., Claeys, M., Gelencser,
626 A., Legrand, M., Preunkert, S., and Pio, C.: Levoglucosan levels at background sites
627 in Europe for assessing the impact of biomass combustion on the European aerosol
628 background, *J. Geophys. Res.: Atmos.*, 16, 112(D23),
629 <https://doi.org/10.1029/2006JD008114>, 2007.
- 630 Reche, C., Viana, M., Amato, F., Alastuey, A., Moreno, T., Hillamo, R., Teinila, K.,
631 Saarnio, K., Seco, R., Penuelas, J., and Mohr, C.: Biomass burning contributions to
632 urban aerosols in a coastal Mediterranean City, *Sci. Tot. Environ.*, 427, 175–190,
633 <https://doi.org/10.1016/j.scitotenv.2012.04.012>, 2012.



- 634 Schauer, J.J., Kleeman, M.J., Cass, G.R., Simoneit, B. R. T.: Measurement of emissions
635 from air pollution sources. 3. C1-C29 organic compounds from fireplace
636 combustion of wood, *Environ. Sci. Technol.*, 35, 1716–1728,
637 <https://doi.org/10.1021/es001331e>, 2001.
- 638 Schmidl, C., Marr, I. L., Caseiro, A., Kotianová, P., Berner, A., Bauer, H., Kasper-Giebl,
639 A., and Puxbaum, H.: Chemical characterisation of fine particle emissions from
640 wood stove combustion of common woods growing in mid-European Alpine
641 regions, *Atmos. Environ.*, 42, 126–141,
642 <https://doi.org/10.1016/j.atmosenv.2007.09.028>, 2008a.
- 643 Shao, M., Czapiewski, K. V., Heiden, A. C., Kobel, K., Komenda, M., Koppmann, R.,
644 and Wildt, J.: Volatile organic compound emissions from Scots pine: mechanisms
645 and description by algorithms, *J. Geophys. Res.: Atmospheres*, 106(D17),
646 20483–20491, [10.1029/2000JD000248](https://doi.org/10.1029/2000JD000248), 2001.
- 647 Sharma, A., Pareek, V., and Zhang, D.: Biomass pyrolysis—A review of modelling,
648 process parameters and catalytic studies. *J. Renew. Sustain. Energy*, 50, 1081–1096,
649 <https://doi.org/10.1016/j.rser.2015.04.193>, 2015.
- 650 Sheesley, R. J., Schauer, J. J., Chowdhury, Z., Cass, G. R., and Simoneit, B. R. T.:
651 Characterization of organic aerosols emitted from the combustion of biomass
652 indigenous to South Asia, *J. Geophys. Res.*, 108, 4285, [http://
653 dx.doi.org/10.1029/2002JD002981](http://dx.doi.org/10.1029/2002JD002981), 2003.
- 654 Simoneit, B. R., Schauer, J. J., Nolte, C. G., Oros, D. R., Elias, V. O., Fraser, M. P., Rogge,
655 W. F., and Cass, G. R., 1999. Levoglucosan, a tracer for cellulose in biomass
656 burning and atmospheric particles, *Atmos. Environ.*, 33, 173–182,
657 [https://doi.org/10.1016/S1352-2310\(98\)00145-9](https://doi.org/10.1016/S1352-2310(98)00145-9), 1999.
- 658 Sullivan, A. P., Guo, H., Schroder, J. C., Campuzano-Jost, P., Jimenez, J. L., Campos, T.,
659 Shah, V., Jaegle, L., Lee, B. H., Lopez-Hilfiker, F. D. and Thornton, J. A.: Biomass
660 Burning Markers and Residential Burning in the WINTER Aircraft Campaign. *J*
661 *Geophys. Res.: Atmos.*, 124, 1846–1861, <https://doi.org/10.1029/2017JD028153>,
662 2019.
- 663 Sullivan, A. P., Holden, A. S., Patterson, L. A., McMeeking, G. R., Kreidenweis, S. M.,
664 Malm, W. C., Hao, W. M., Wold, C. E., and Collett Jr., J. L.: A method for smoke
665 marker measurements and its potential application for determining the contribution



- 666 of biomass burning from wildfires and prescribed fires to ambient PM_{2.5} organic
667 carbon, *J Geophys. Res.*, 113, D22302, [http:// dx.doi.org/10.1029/2008JD010216](http://dx.doi.org/10.1029/2008JD010216),
668 2008.
- 669 Tai, A. P., Mickley, L. J., and Jacob, D. J.: Correlations between fine particulate matter
670 (PM_{2.5}) and meteorological variables in the United States: Implications for the
671 sensitivity of PM_{2.5} to climate change, *Atmos. Environ.*, 44, 3976-3984,
672 <https://doi.org/10.1016/j.atmosenv.2010.06.060>, 2010.
- 673 Tao, J., Zhang, L., Ho, K., Zhang, R., Lin, Z., Zhang, Z., Lin, M., Cao, J., Liu, S., and
674 Wang, G.: Impact of PM_{2.5} chemical compositions on aerosol light scattering in
675 Guangzhou—the largest megacity in South China, *Atmos. Res.*, 135, 48–58,
676 <https://doi.org/10.1016/j.atmosres.2013.08.015>, 2014.
- 677 Thepnuan, D., Chantara, S., Lee, C. T., Lin, N. H., and Tsai, Y. I.: Molecular markers for
678 biomass burning associated with the characterization of PM_{2.5} and component
679 sources during dry season haze episodes in Upper South East Asia. *Sci. Tot.*
680 *Environ.*, 658, 708–722, <https://doi.org/10.1016/j.scitotenv.2018.12.201>, 2019.
- 681 Verma, V., Fang, T., Guo, H., King, L., Bates, J. T., Peltier, R. E., Edgerton, E., Russell,
682 A. G., and Weber, R. J.: Reactive oxygen species associated with water-soluble
683 PM_{2.5} in the southeastern United States: spatiotemporal trends and source
684 apportionment, *Atmos. Chem. Phys.*, 14, 12915-12930,
685 <https://doi.org/10.5194/acp-14-12915-2014>, 2014.
- 686 Wang, T., Tian, M., Ding, N., Yan, X., Chen, S. J., Mo, Y. Z., Yang, W. Q., Bi, X. H.,
687 Wang, X. M., and Mai, B. X.: Semivolatile organic compounds (SOCs) in fine
688 particulate matter (PM_{2.5}) during clear, fog, and haze episodes in winter in Beijing,
689 China, *Environ. Sci. Tech.*, 52, 5199–5207, <https://doi.org/10.1021/acs.est.7b06650>,
690 2018.
- 691 Watson, J. G., Chow, J. C., and Fujita, E. M.: Review of volatile organic compound source
692 apportionment by chemical mass balance, *Atmos. Environ.*, 35, 1567–1584,
693 [https://doi.org/10.1016/S1352-2310\(00\)00461-1](https://doi.org/10.1016/S1352-2310(00)00461-1), 2001a.
- 694 Watson, J. G., Chow, J. C., and Houck, J. E.: PM_{2.5} chemical source profiles for vehicle
695 exhaust, vegetative burning, geological material, and coal burning in Northwestern
696 Colorado during 1995, *Chemosphere*, 43, 1141–1151,
697 [https://doi.org/10.1016/S0045-6535\(00\)00171-5](https://doi.org/10.1016/S0045-6535(00)00171-5), 2001b.



- 698 Zhang, F., Wang, Z. W., Cheng, H. R., Lv, X. P., Gong, W., Wang, X. M., and Zhang, G.:
699 Seasonal variations and chemical characteristics of PM_{2.5} in Wuhan, central China,
700 *Sci. Tot. Environ.*, 518, 97–105, <https://doi.org/10.1016/j.scitotenv.2015.02.054>,
701 2015.
- 702 Zhang, Y. X., Min, S., Zhang, Y. H., Zeng, L. M., He, L. Y., Bin, Z. H. U., Wei, Y. J., and
703 Zhu, X. L.: Source profiles of particulate organic matters emitted from cereal straw
704 burnings. *J Environ. Sci.*, 19, 167–175, [https://doi.org/10.1016/S1001-](https://doi.org/10.1016/S1001-0742(07)60027-8)
705 [0742\(07\)60027-8](https://doi.org/10.1016/S1001-0742(07)60027-8), 2007.
- 706 Zhou, Y., Levy, J. I., Hammitt, J. K., and Evans, J. S.: Estimating population exposure to
707 power plant emissions using CALPUFF: a case study in Beijing, China, *Atmos.*
708 *Environ.*, 37, 815–826, [https://doi.org/10.1016/S1352-2310\(02\)00937-8](https://doi.org/10.1016/S1352-2310(02)00937-8), 2003.
- 709 Zhu, C., Kawamura, K., and Kunwar, B.: Effect of biomass burning over the western
710 North Pacific Rim: wintertime maxima of anhydrosugars in ambient aerosols from
711 Okinawa, *Atmos. Chem. Phys.*, 15, 1959–1973, [https://doi.org/10.5194/acp-15-](https://doi.org/10.5194/acp-15-1959-2015)
712 [1959-2015](https://doi.org/10.5194/acp-15-1959-2015), 2015.



Table 1. Concentrations ($\mu\text{g m}^{-3}$) of organic carbon, elemental carbon, levoglucosan, mannosan, galactosan, and water-soluble ions in $\text{PM}_{2.5}$ samples collected from Ulaanbaatar, Mongolia, during the winter ($n = 17$) and spring ($n = 17$) of 2017.

	OC	EC	Levoglucosan	Mannosan	Galactosan	Cl ⁻	SO ₄ ²⁻	NO ₃ ⁻	Na ⁺	NH ₄ ⁺	K ⁺	Mg ²⁺	Ca ²⁺	Temperature (°C)	Wind Speed (m sec ⁻¹)	RH (%)
Winter																
Mean	49.06	1.71	1.20	0.33	0.24	1.69	9.74	4.17	0.64	6.18	0.13	0.05	0.60	-20.8	1.36	66.1
SD	17.32	0.58	0.43	0.13	0.09	0.76	3.37	1.69	0.44	2.42	0.04	0.02	0.24	4.74	0.73	4.56
Min	24.62	0.79	0.58	0.15	0.10	0.26	2.17	0.76	0.10	3.16	0.08	0.02	0.22	-27.8	0.41	58.5
Max	79.07	3.34	2.12	0.61	0.43	2.89	16.06	7.51	1.34	11.59	0.18	0.08	1.04	-10.5	3.55	72.7
Spring																
Mean	8.50	1.11	0.31	0.08	0.04	0.30	1.90	0.70	0.13	0.74	0.08	0.04	0.93	6.11	2.60	35.1
SD	3.55	0.42	0.18	0.04	0.02	0.11	0.50	0.32	0.04	0.28	0.05	0.02	0.36	6.16	0.79	13.9
Min	2.80	0.60	0.03	0.01	0.00	0.11	1.04	0.10	0.07	0.33	0.02	0.02	0.48	-1.52	1.64	17.8
Max	16.63	2.03	0.73	0.15	0.08	0.51	3.02	1.40	0.21	1.47	0.22	0.08	1.61	15.9	4.56	65.2



Table 2. Source identification of chemical species using principal component (PC) analysis and varimax rotation at Ulaanbaatar, Mongolia, during winter of 2017.

Chemical species	Component			
	PC1 (Biomass Burning)	PC2 (Dust)	PC3 (Secondary formation)	PC4 (Vehicular)
Levogluconan	0.96	-0.06	0.24	0.06
Mannosan	0.95	-0.08	0.27	0.06
Galactosan	0.95	-0.07	0.28	0.04
Cl ⁻	0.19	0.94	-0.05	-0.07
SO ₄ ²⁻	0.43	0.01	0.88	0.09
NO ₃ ⁻	0.28	0.20	0.87	0.20
Na ⁺	-0.27	0.87	-0.33	-0.17
NH ₄ ⁺	0.48	-0.12	0.86	0.07
K ⁺	0.70	0.11	0.61	0.25
Mg ₂ ⁺	-0.15	0.90	0.25	0.26
Ca ₂ ⁺	-0.12	0.92	0.19	0.24
OC	0.82	-0.17	0.47	0.07
EC	0.14	0.14	0.19	0.95
Eigenvalues	4.54	3.44	3.30	1.20
% of Variance	34.95	26.49	25.37	9.21
Cumulative %	34.95	61.44	86.81	96.02



Table 3. Source identification of chemical species using PCA and varimax rotation at Ulaanbaatar, Mongolia, during spring of 2017.

Chemical species	Spring		
	PC1 (Biomass Burning)	PC2 (Dust and Vehicular)	PC3 (Secondary formation)
Levogluconan	0.88	0.13	0.39
Mannosan	0.94	0.00	0.30
Galactosan	0.95	-0.11	0.20
Cl ⁻	0.81	0.32	-0.03
SO ₄ ²⁻	0.18	0.12	0.93
NO ₃ ⁻	0.59	0.54	0.52
Na ⁺	0.08	0.91	-0.09
NH ₄ ⁺	0.44	0.05	0.88
K ⁺	0.41	0.67	0.55
Mg ²⁺	0.05	0.90	0.35
Ca ²⁺	0.10	0.97	0.15
OC	0.77	0.41	0.46
EC	0.10	0.94	0.01
Eigenvalues	4.59	4.53	2.87
% of Variance	35.30	34.84	22.04
Cumulative %	35.30	70.14	92.18



Table 4. Correlation coefficients (r) from Spearman correlation analysis for $OC_{\text{non-BB}}$ and water-soluble ions during winter and spring of 2017 at Ulaanbaatar, Mongolia.

	Cl^-	SO_4^{2-}	NO_3^-	Na^+	NH_4^+	K^+	Mg^{2+}	Ca^{2+}	EC
Winter	-0.26	0.71**	0.44	-0.58*	0.72**	0.64**	-0.16	-0.16	0.15
Spring	0.29	0.37	0.59*	0.74**	0.23	0.65**	0.78**	0.77**	0.74**

*Correlation is significant at the .05 level (2-tailed); **Correlation is significant at the .01 level (2-tailed).



Figure captions

- Fig. 1 Sampling site in Ulaanbaatar, Mongolia (<https://www.google.com/earth/versions/#earth-pro>). ©Google Earth.
- Fig. 2 Daily variations in atmospheric concentrations ($\mu\text{g m}^{-3}$) of chemical species in Ulaanbaatar during winter (a) and spring (b) of 2017.
- Fig. 3 Daily atmospheric concentrations of OC ($\mu\text{g C m}^{-3}$) as a function of wind speed (m s^{-1}) and temperature ($^{\circ}\text{C}$) during winter (a) and spring (b) of 2017.
- Fig. 4 Relationship between $\text{PM}_{2.5}$ concentrations of Ca^{2+} and EC ($\mu\text{g m}^{-3}$) and temperature ($^{\circ}\text{C}$) during spring of 2017.
- Fig. 5 (a) Five-day backward air-mass trajectories (<https://ready.arl.noaa.gov/HYSPLIT.php>) and (b) FIRMS fire counts (<https://firms.modaps.eosdis.nasa.gov/alerts/>) around Ulaanbaatar during spring of 2017.
- Fig. 6 Correlations of $\text{PM}_{2.5}$ concentrations ($\mu\text{g m}^{-3}$) of mannosan and galactosan with levoglucosan during winter (a) and spring (b) of 2017.
- Fig. 7 Correlation between $\text{PM}_{2.5}$ concentrations of (a) OC ($\mu\text{g C m}^{-3}$) and levoglucosan ($\mu\text{g m}^{-3}$) and (b) K^{+} and levoglucosan ($\mu\text{g m}^{-3}$) in during winter and spring of 2017.
- Fig. 8 Correlation between $\text{PM}_{2.5}$ concentrations of OC ($\mu\text{g C m}^{-3}$) and K^{+} ($\mu\text{g m}^{-3}$) during winter (a) and spring (b) of 2017.
- Fig. 9 Scatter plot of levoglucosan/ K^{+} versus levoglucosan/mannosan from different types of BB emissions, including those measured in Ulaanbaatar (blue circles and red squares).



- Fig. 10. Comparison of previously reported OC/levoglucosan ratios for softwood burning.
- Fig. 11 Graphical determination of optimized OC/levoglucosan ratios used to estimate OC_{BB} in Ulaanbaatar in winter (a) and spring (b) of 2017.
- Fig. 12 Relative contributions ($\mu\text{g C m}^{-3}$) of OC_{BB} and OC_{non-BB} to $PM_{2.5}$ in Ulaanbaatar during winter and spring of 2017.



Fig. 1

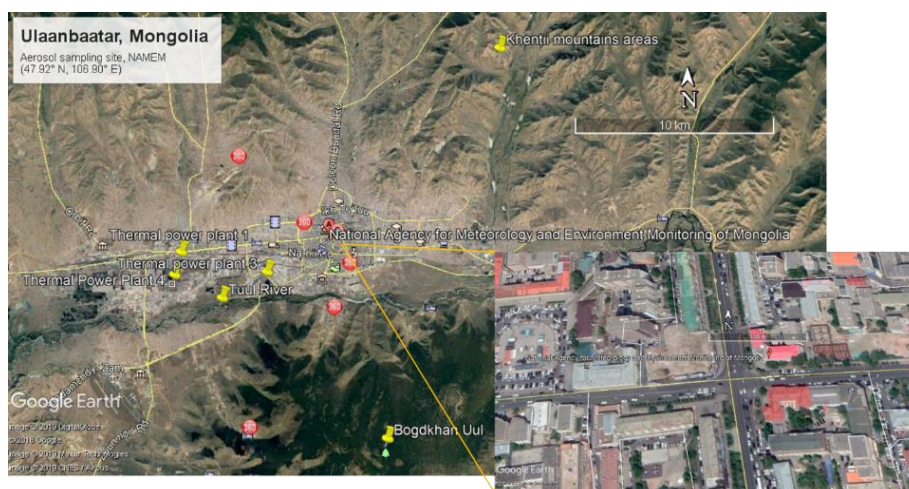




Fig. 2

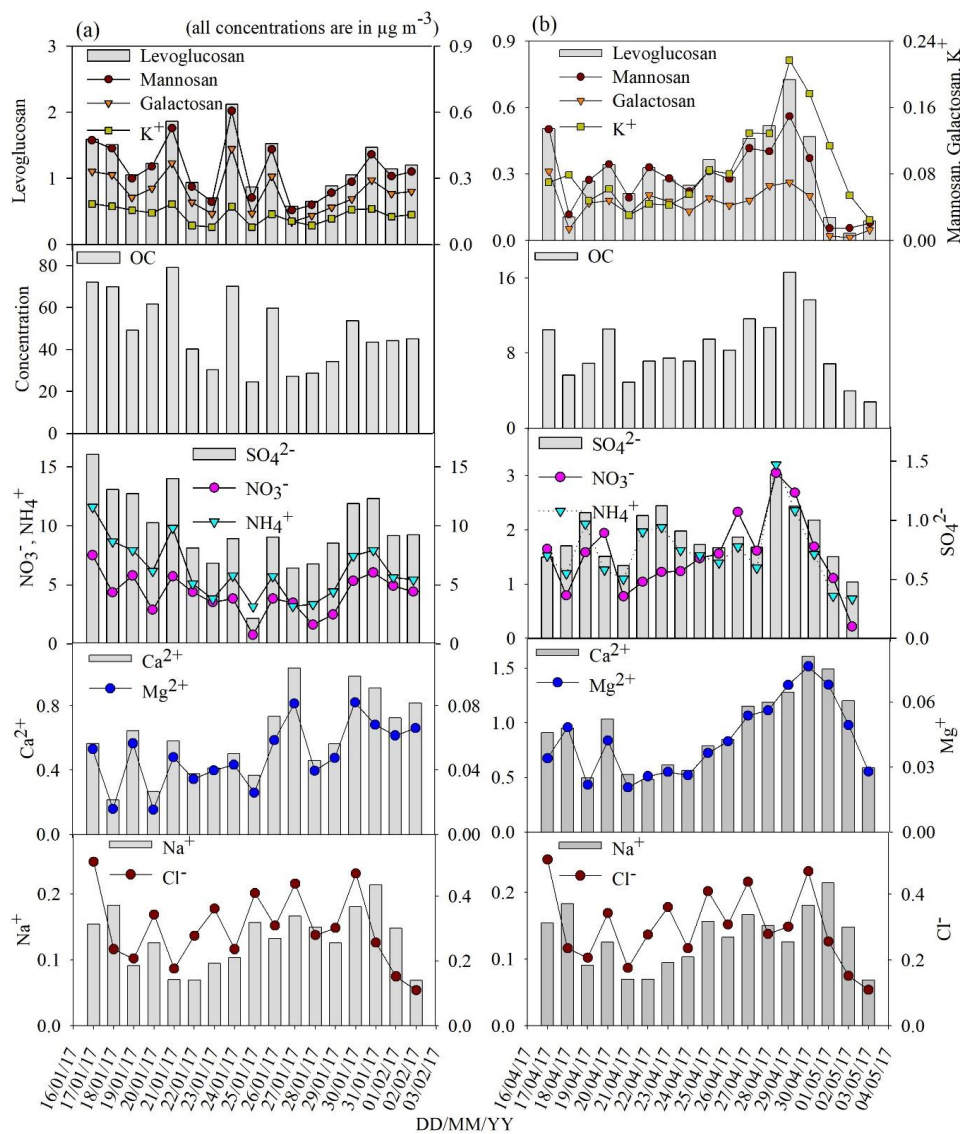




Fig. 3

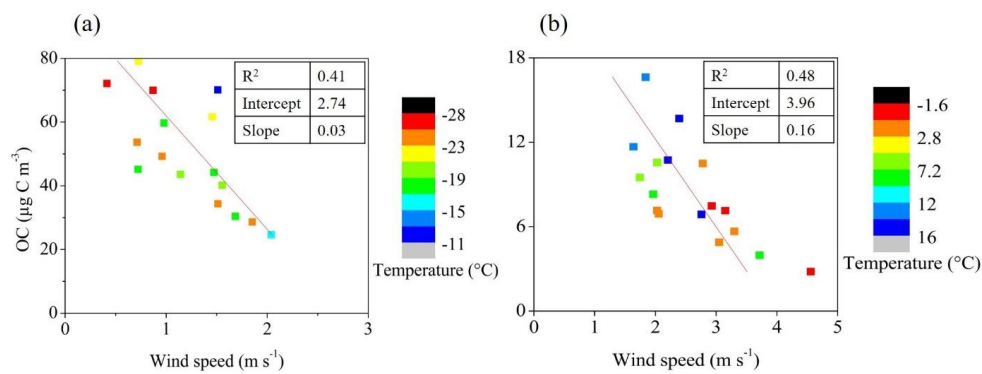




Fig. 4

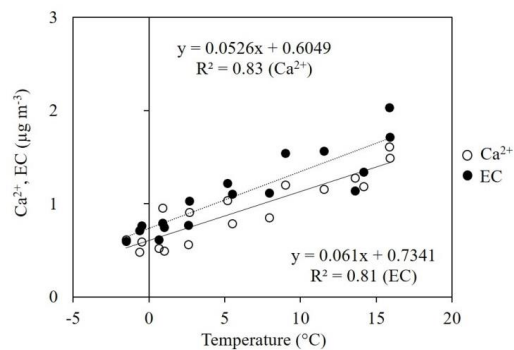




Fig. 5

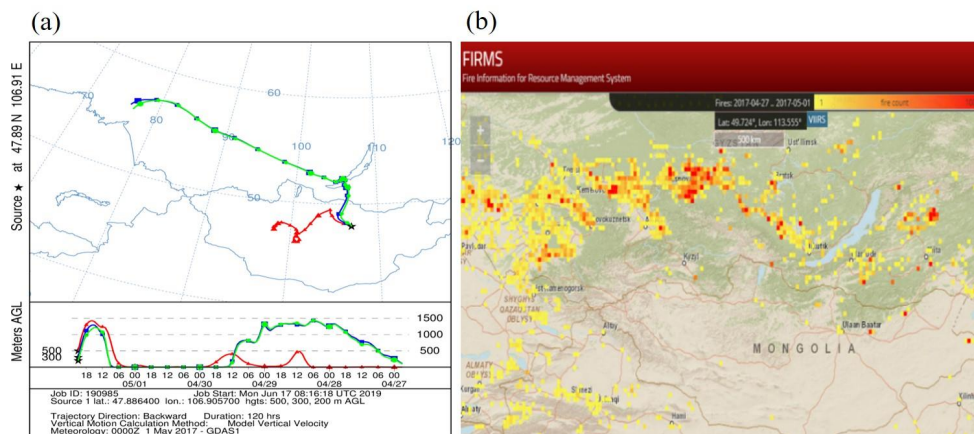
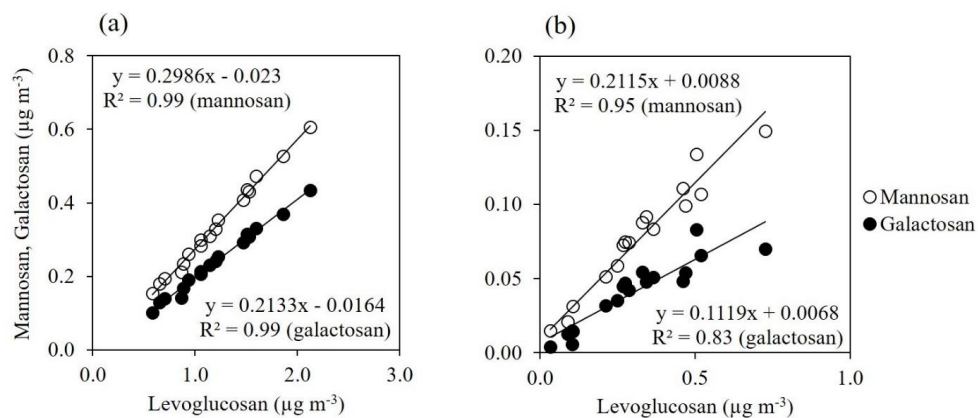




Fig. 6



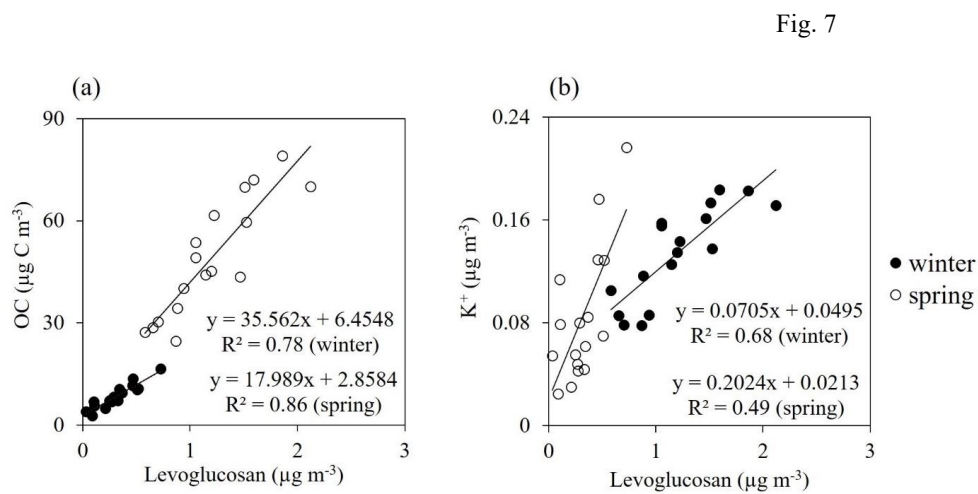




Fig. 8

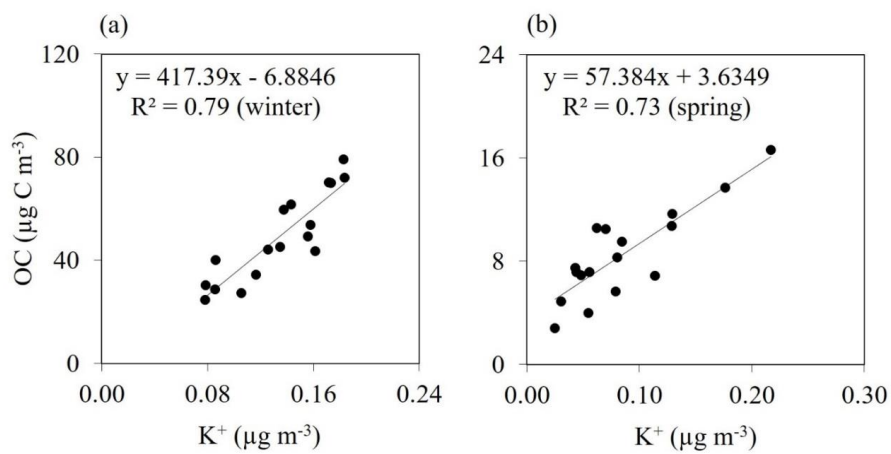




Fig. 9

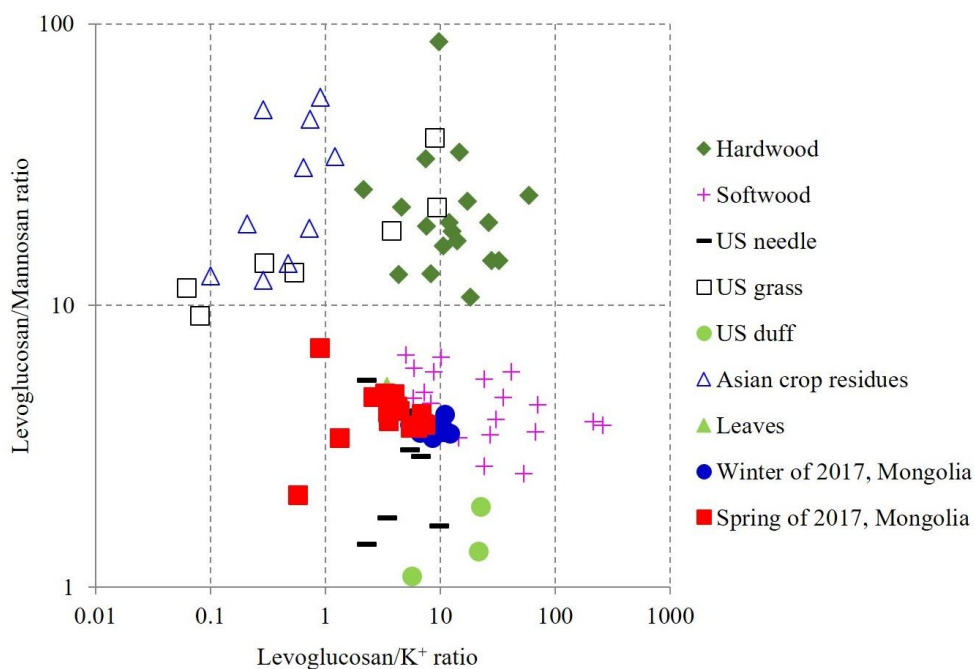




Fig. 10

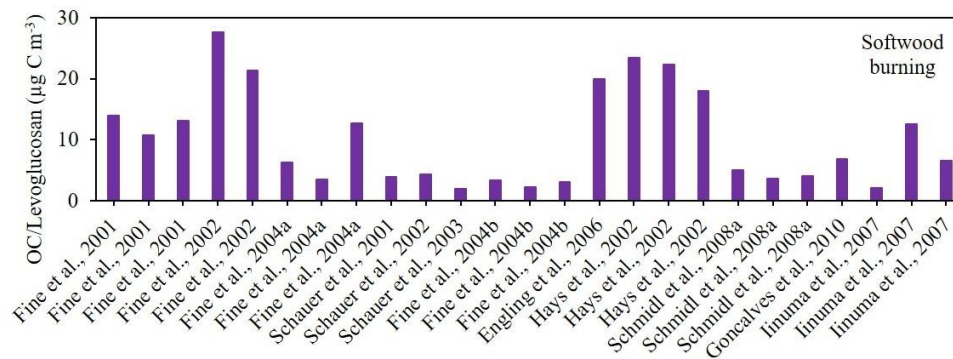




Fig. 11

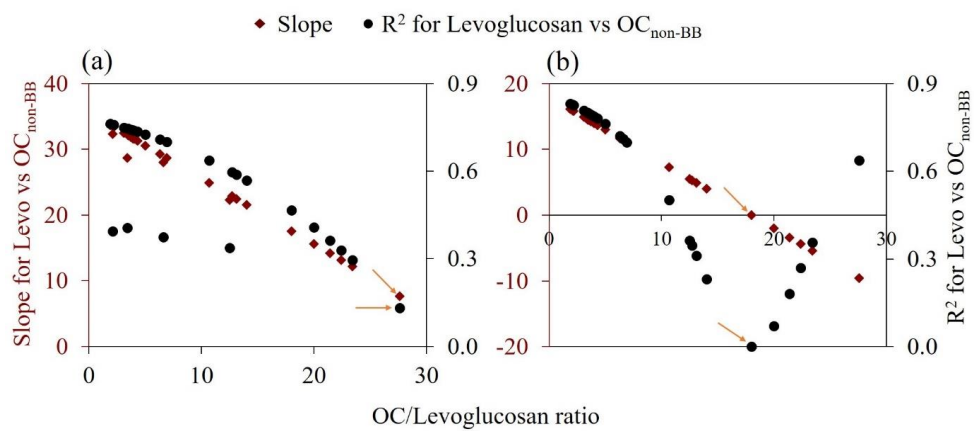




Fig. 12

